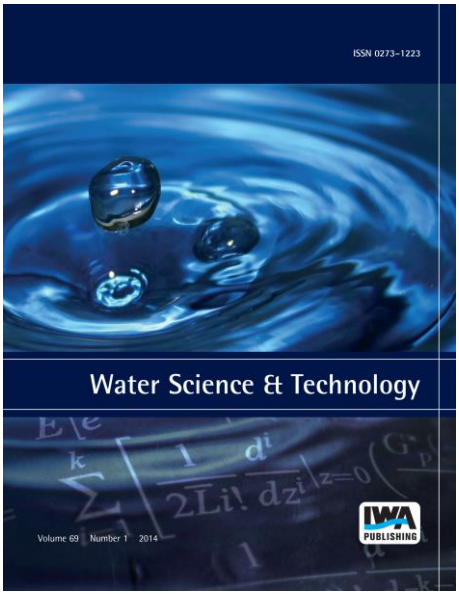

The adsorption and Fenton behavior of iron rich Terra Rosa soil for removal of aqueous anthraquinone dye solutions: kinetic and thermodynamic studies

Doga Aktas, Nadir Dizge, H. Cengiz Yatmaz, Yasemin Caliskan, Yasin Ozay and Ayten Caputcu

ABSTRACT

Adsorption and advanced oxidation processes are being extensively used for treatment of wastewater containing dye chemicals. In this study, the adsorption and Fenton behavior of iron rich Terra Rosa soil was investigated for the treatment of aqueous anthraquinone dye (Reactive Blue 19 (RB19)) solutions. The impact of pH, initial dye concentration, soil loading rate, contact time and temperature was systematically investigated for adsorption process. A maximum removal efficiency of dye (86.6%) was obtained at pH 2, soil loading of 10 g/L, initial dye concentration of 25 mg/L, and contact time of 120 min. Pseudo-first-order, pseudo-second-order, Elovich, and Weber–Morris kinetic models were applied to describe the adsorption mechanism and sorption kinetic followed a pseudo-second-order kinetic model. Moreover, Langmuir, Freundlich and Temkin isotherm models were used to investigate the isothermal mechanism and equilibrium data were well represented by the Langmuir equation. The maximum adsorption capacity of soil was found as 4.11 mg/g using Langmuir adsorption isotherm. The effect of soil loading and hydrogen peroxide (H_2O_2) dosage was solely tested for Fenton oxidation process. The highest removal efficiency of dye (89.4%) was obtained at pH 2, H_2O_2 dosage of 10 mM, soil loading of 5 g/L, initial dye concentration of 50 mg/L, and contact time of 60 min. Thermodynamic studies showed that when the adsorption dosage of dye was 25 mg/L at 293–313 K, adsorption enthalpy (ΔH) and entropy (ΔS) were negative and adsorption free energy (ΔG) was positive. This result indicated that the adsorption was exothermic. Morphological characteristics of the soil were evaluated by X-ray fluorescence (XRF), scanning electron microscopy (SEM), and attenuated total reflection Fourier transform infrared (ATR-FTIR) spectroscopy before and after the adsorption and oxidation process.

Key words | adsorption kinetics, Fenton oxidation, Reactive Blue 19, Terra Rosa soil, thermodynamic

Doga Aktas
Nadir Dizge (corresponding author)
Yasin Ozay
Department of Environmental Engineering,
Mersin University,
33343 Yenisehir,
Mersin,
Turkey
E-mail: *nadirdizge@gmail.com*

H. Cengiz Yatmaz
Yasemin Caliskan
Department of Environmental Engineering,
Gebze Technical University,
41400 Gebze,
Kocaeli,
Turkey

Ayten Caputcu
Department of Geology Engineering,
Mersin University,
33343 Yenisehir,
Mersin,
Turkey

INTRODUCTION

Water pollution is a growing environmental problem and different solutions should be found to protect environmental resources. On the other hand, water pollution is continuously increasing and extensive scientific efforts are carried out to solve the environmental problems worldwide. Numerous industrial activities yield water pollution and the textile industry consumes a substantial amount of water resources during the production process and discharges low degradability wastes. The textile sector produces wastewater with several harmful contaminants, i.e. toxic compounds, acidic–caustic chemicals and several dyes (Al-Ghouti *et al.* 2003). Dye chemicals deliver environmental risks, especially to human health, aquatic species and micro-organisms because of their carcinogenic, mutagenic, teratogenic, and toxic properties (Guaratini & Zanoni 2000). Colored compounds affect the nature of water and inhibit sunlight penetration as well as reduce photosynthetic activity (Sivaraj *et al.* 2001). Anthraquinone dyes are the second most important class of dyes used by the textile industry and locate considerable importance in textile effluents. In contrast to the azo dyes, which have no natural counterparts, the anthraquinone chromogen provides all the important natural red dyes (Gordon & Gregory 1987).

doi: 10.2166/wst.2017.468

Adsorption technologies were associated with low cost and high efficiency processes in the treatment of different kinds of industrial wastewater due to the high affinity for removing of organic matters (Bangash & Alam 2009; Ncibi *et al.* 2009). Until now, extensive amount of studies has been performed to find low-cost adsorbents such as wood chips, peat, cow dung ash, sugarcane bagasse, ash char, rice husk residue, and coconut residual fiber (Low *et al.* 2000; Moreira *et al.* 2001; Allen *et al.* 2004; Rattan *et al.* 2008; Silva *et al.* 2011; Li *et al.* 2016; Rani *et al.* 2017). The use of soils as an adsorbent for the treatment of wastewater is a potential alternative material to conventional treatments (Fil *et al.* 2014; Murali *et al.* 2015; Russiarani & Balakrishanan 2015). Terra Rosa soil generally includes clay minerals such as Kaolinite-Montmorillonite-Illite and iron oxides minerals such as hematite-goethite, quartz and feldspar minerals (Bronger *et al.* 1983; Torrent & Cabedo 1986; Boero & Schwertmann 1989; Boero *et al.* 1992; Durn *et al.* 1999).

In this study, Terra Rosa soil was investigated as a low-cost adsorbent for the removal of Reactive Blue 19 (RB19) dye which is widely used in textile industries. Sorption experiments were carried out for adsorption kinetics and equilibrium studies. The factors affecting the sorption process such as pH, initial dye concentration, soil loading, contact time, and temperature were investigated. Pseudo-first-order, pseudo-second-order, Elovich, and Weber–Morris kinetic models were used to describe the adsorption mechanism. Langmuir, Freundlich, and Temkin isotherm models were performed to the experimental data. Meantime, Fenton studies were also performed using different soil loading and H_2O_2 dosage. X-ray fluorescence (XRF), scanning electron microscopy (SEM) and attenuated total reflection Fourier transform infrared (ATR-FTIR) spectroscopy were evaluated for soil characterization before and after the adsorption and oxidation process.

MATERIALS AND METHODS

Geography and geology of soil

Terra Rosa soil is collected from the location at the northern parts of Mersin City (Figure 1). The soil was sampled in the surface layers (0–20 cm). The average of annual moisture content is about 62% at the region which has average annual temperature of 19.1 °C and total annual rainfall of 592 mm. Soil which develops on the different source of limestone, attention-grabbing with red color and clay are called 'Red Mediterranean Soils' or 'Terra Rosa' (Kubiena 1953; Yaalon 1997; Günal 2006). Iron hydroxides in the soil lose the water from their structure because of the seasonally lack of water caused from climatic conditions. Iron oxides which develop as the result of water loss, supply red color to the soil with covering clay and other particles (Yaalon 1997; Günal 2006).

The soil was washed with distilled water several times to remove all the dirty particles adhering to the surface. The washed adsorbents were dried in an oven at 105 °C for 24 h. Then, the dried soil was grounded and sieved to obtain the particle size of 250 μm. Finally, the soil samples were stored in an airtight container.

Dye specifications and solution preparation

The anthraquinone dye, Remazol Brilliant Blue R (Reactive Blue 19) (Color Index Number 61200), was obtained from Sigma-Aldrich. The characterization of the dye is presented in Table 1.

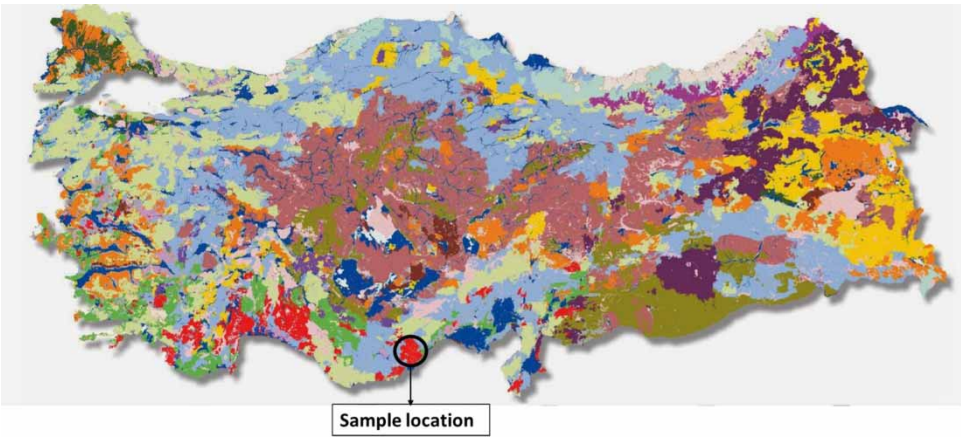

Figure 1 | Collected soil samples location (http://agitkavak.blogspot.com/2013/12/turkiye-fiziki-cografya-atlasi.html).

The stock solution of RB19 dye (500 mg/L) was prepared by dissolving 0.5 g of dye in 1,000 mL of deionized water. Tap water was purified in the laboratory by means of a Milli-Q system (Millipore). The required lower concentrations (25, 50, 100 mg/L) were prepared by dilution of the stock solution. Hydrochloric acid (HCl) and sodium hydroxide (NaOH) were used for pH adjustment. The pH measurements were carried out with a glass electrode (Hach Lange HQ40d Model pH meter).

A UV/VIS Spectrometer (T + 90, PG Instruments Ltd) was used to analyze the concentration of dye in solutions at 590 nm. Calibration curves were prepared between 5 and 200 mg/L. Precision of the parallel measurements was as ±2%SD.

Data analysis

The amount of RB19 adsorbed by the Terra Rosa soils, q_e (mg/g), was calculated by Equation (1):

$$\text{Adsorption capacity } (q_e) = \frac{(C_o - C_e)\,V}{m} \quad (1)$$

The dye removal percentage was calculated by Equation (2):

$$\text{Color removal } (\%) = \frac{C_0 - C_e}{C_0} \times 100 \quad (2)$$

Table 1 | Physico-chemical specifications of RB19 dye

Specification	Remazol Brilliant Blue R
Chemical structure	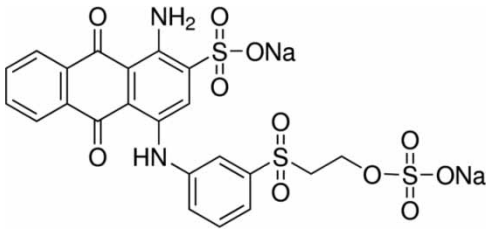
Molecular formula	$C_{22}H_{16}N_2Na_2O_{11}S_3$
Synonym	Reactive Blue 19
Appearance	Crystalline powder
Solubility	Soluble in water
Dye content	~50%
Molecular weight	626.54 g mol^{-1}
Max. wavelength	590 nm

where C_0 and C_e are the initial and equilibrium concentrations of RB19 in solution (mg/L), respectively. V is the total volume of the RB19 solution (L), and m is the mass of Terra Rosa soil (g).

Adsorption kinetic and isotherm studies

Adsorption kinetic

In this study, pseudo-first-order, pseudo-second-order, Elovich, and Weber–Morris equations were used to describe the adsorption mechanism.

The pseudo-first-order model equation is:

$$\log(q_e - q_t) = \log(q_e) - \frac{k_1}{2.303}(t) \quad (3)$$

where q_e (mg/g) is the amount of adsorbed dye at the point of equilibrium, q_t (mg/g) is the amount of adsorbed dye at time t, and k_1 (min^{-1}) is the rate constant which can be calculated from the straight-line plot of $\log(q_e\text{-}q_t)$ vs t.

The pseudo-second-order model equation is:

$$\frac{t}{q_t} = \frac{1}{k_2 q_e^2} + \frac{1}{q_e}(t) \quad (4)$$

where q_e (mg/g) is the amount of adsorbed dye at the equilibrium time, q_t (mg/g) is the amount of adsorbed dye at time t, and k_2 (min^{-1}) is the rate constant which can be calculated from the straight-line plot of t/q_t vs t.

The Elovich model equation is:

$$q_t = \frac{1}{\beta}\ln(\alpha\beta) + \frac{1}{\beta}\ln(t) \quad (5)$$

where α is the initial adsorption rate (mg/g·min) and β is the desorption constant (g/mg) which can be calculated from the straight-line plot of q_t vs ln(t).

The Weber–Morris model equation is:

$$q_t = k_{id}\, t^{1/2} + I \quad (6)$$

where q_t (mg/g) is the amount of adsorbed dye at time t, k_{id} (mg/g·$min^{1/2}$) is the rate constant for intraparticle diffusion and I is intercept which can be calculated from the straight-line plot of q_t vs $t^{1/2}$.

Adsorption isotherm

In this study, Langmuir, Freundlich, and Temkin equations were used to investigate the isothermal mechanism on the

adsorption process. The Langmuir equation is designed to homogeneous sorption, while the Freundlich equation is applicable to heterogeneous sorption.

The Langmuir isotherm equation is:

$$\frac{C_e}{q_e} = \frac{1}{Q_o b} + \frac{C_e}{Q_o} \tag{7}$$

where C_e (mg/L) is the concentration of dye at equilibrium; q_e is the amount of absorbed dye at time; Q_o (mg/g) is the maximum adsorption capacity; b is the Langmuir rate constant which can be calculated from the straight-line plot of C_e/q_e vs. C_e.

The Freundlich isotherm equation is:

$$\log q_e = \log k_F + \left(\frac{1}{n}\right) \log C_e \tag{8}$$

where C_e (mg/L) is the concentration of dye at equilibrium; q_e is the amount of absorbed dye at time; k_F and n are the Freundlich rate constant which can be calculated from the straight-line plot of log q_e vs. log C_e.

The Temkin isotherm equation is:

$$q_e = B \ln A + B \ln C_e \tag{9}$$

where C_e (mg/L) is the concentration of dye at equilibrium; q_e is the amount of dyes absorbed at time; A (L/g) is Temkin equilibrium binding constant; and B $(= RT/b)$(J/mol) is Temkin constant related to heat of sorption which can be calculated from the straight-line plot of q_e vs. ln C_e. However, R is universal gas constant (8.314 J/mol·K), T is temperature (K), b is Temkin isotherm constant.

Adsorption kinetic and isotherm studies on Terra Rosa soil were performed in batch experiments. A desired amount of the adsorbent was weighed into a 500-mL glass stoppered conical flask. The experimental parameters such as pH (1–10), soil loading (2.5–20 g/L), initial dye concentration (25–100 mg/L), and contact time (0–120 min) were evaluated for 250-mL RB19 solution (Table 2). The flasks were shaken (300 rpm) for 120 min at 25 ± 1 °C. A thermostated shaker of orbital model (KS-15, Edmund Bühler GmbH) incubator was used for adsorption and temperature experiments. Samples were analyzed versus time to determine residual dye concentration. Samples were separated by centrifugation (6,000 rpm, 5 min) before analysis. All samples were tested in triplicate and average values were presented.

In addition, adsorption isotherm was also studied at different temperatures ranging from 298 to 313 K using the thermostat orbital shaker. The soil was centrifuged and residual dye concentration in solution was measured after being equilibrated for 180 min.

Adsorption thermodynamic studies

For thermodynamic studies, RB19 solution (25 mg/L, 250-mL) containing conical flasks were placed on a rotary shaker (300 rpm) at different temperatures (25, 30, 40 °C). Samples were withdrawn periodically for residual RB19 concentration analysis.

Heterogeneous Fenton studies

The experiments were carried out in a 500-mL conical flask containing 250-mL of dye solution at pH 2.0 and dye concentration of 50 mg/L. The effect of soil loading and hydrogen peroxide (H_2O_2) dosage was tested for Fenton oxidation process. All the experiments were carried out under constant shaking (300 rpm) for 60 min at 25 ± 1 °C. Samples were analyzed versus time to determine residual dye concentration. Samples were separated by centrifugation (6,000 rpm, 5 min) before analysis. All samples were tested in triplicate and average values were presented.

Table 2 | Experimental conditions for RB19 dye adsorption on Terra Rosa soil

		Conditions			
Exp. run	**Tested parameter**	**pH**	**Soil loading (g/L)**	**Initial dye concentration (mg/L)**	**Contact time (min)**
1	Effect of pH	1–10	10	25	120
2	Effect of soil loading	2	2.5–20	25	120
3	Effect of initial dye concentration	2	10	25–100	120
4	Effect of contact time	2	10	25–100	1–120
4	Equilibrium tests	2	10	25–200	180

Soil characterization and analytical methods

The surface of soil was characterized by SEM (Zeiss/Supra 55 FE-SEM) before and after the adsorption experiments. All samples were dried and coated under vacuum with gold by a sputtering system.

XRF analyses were carried out by Thermo-Scientific and the soil samples were dried, homogenized, and sieved at 250 μm particle sizes. The XRF intensity will saturate at a certain soil thickness. The X-ray tube was operated at 40 kV, 0.3 mA for 240 s. The sample name, spectrum, and elemental composition are found in a dedicated library.

The ATR-FTIR (Perkin Elmer) spectra of samples were collected at room temperature in the range of 450– 4,000 cm^{-1}.

Iron concentration was also measured using inductively coupled plasma optical emission spectrometry (ICP-OES) (Optima 7000 DV, PerkinElmer).

RESULTS AND DISCUSSION

Adsorption kinetic analysis of RB19 dye from aqueous solution

Effect of pH

The adsorption phenomena on solid surfaces are closely related with solution pH ranges from acidic to alkaline. For this reason, the effect of pH on the sorption of RB19 dye was tested at different pH values (1–10) using Terra Rosa soil at constant dye concentration (25 mg/L) and soil loading (10 g/L) (in the first row of Table 2). As shown in Figure 2, the highest dye removal (86.6%) was obtained at pH 2. Therefore, all the adsorption experiments were carried out at pH 2. However, dye sorption capacity of the soil decreased from 15.6% to 3.7% with increase of pH from 3 to 10, respectively. The results showed that the adsorption process is pH-dependent due to the surface characteristics of soil. The surface charge of Terra Rosa soil was also changed with pH, going from positive in the acidic pH region to zero at the pH_{pzc} around pH 3 and then negative at higher pH values. Zeta potential of soil was measured as 1.38 ± 0.35 and -30.31 ± 0.12 mV at pH 2 and pH 10, respectively. In low pH, the surface of soil material was charged with H^+ ion and this leads to a strong electrostatic attraction between the positively charged soil surface and negatively charged dye molecules ($-SO_3^{-2}$), which caused an increasing rate in dye sorption (Ho *et al.* 2002).

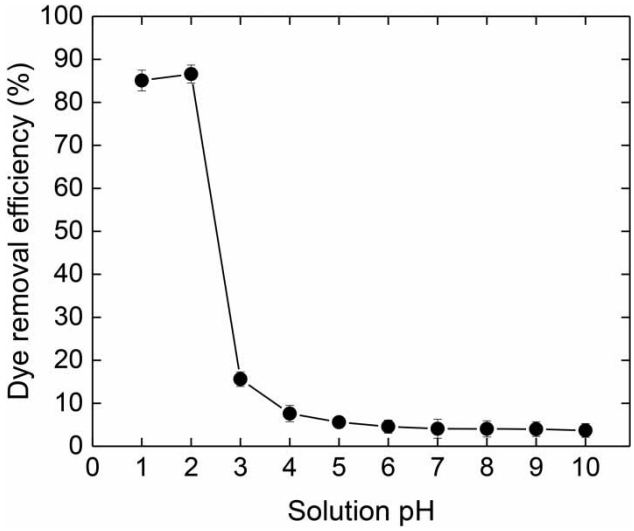

Figure 2 | Effect of solution pH (1–10) on the RB19 dye removal by Terra Rosa soil (adsorbent dose, 10 g/L; initial dye concentration, 25 mg/L; contact time, 120 min).

Effect of Terra Rosa soil loading

The effect of soil loading on RB19 dye removal was tested at an optimum pH of 2 (in the second row of Table 2). Figure 3 shows the removal percentages of dye as a function of soil dosage. As represented in Figure 3, the removal of dye at doses of 2.5, 5.0, 10, 15, 20 g/L was 38.2, 73.5, 86.6, 86.6, 86.7%, respectively. The results showed that dye removal efficiency improved up to 10 g/L soil dosage and remained almost unchanged between 10–20 g/L of soil dosage. This

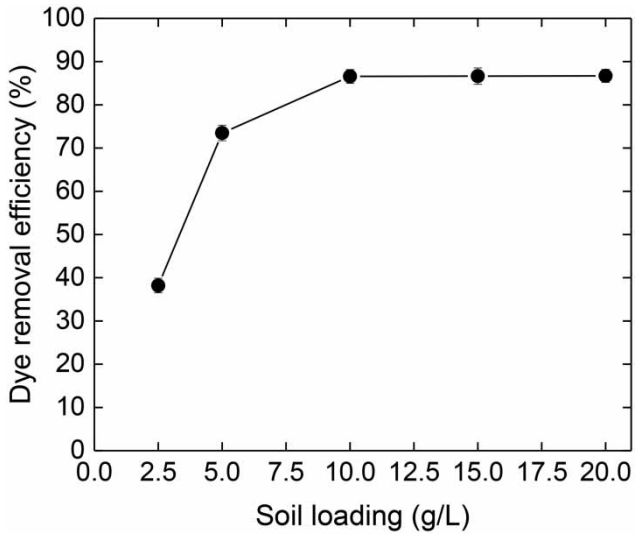

Figure 3 | Effect of soil loading (2.5–20 g/L) on the RB19 dye removal by Terra Rosa soil (pH, 2; initial dye concentration, 25 mg/L; contact time, 120 min).

may be because lower soil loading supplied higher active sites. In addition, with the increase in soil loading can affect aggregation of particles which decreases in total adsorbent surface area of particles, as a result efficiency and dye uptake decreases. The aggregation may also influence an increase in diffusion path length. For this reason, 10 g/L of soil dosage was selected as an optimum value for the further experiments.

Effect of initial dye concentration and agitation time

Dye concentration was studied in the range of 25 to 100 mg/L at an optimum pH of 2 and adsorbent dosage of 10 g/L (in the third row of Table 2). Dye removal efficiency reached the maximum value of 86.6, 58.9, 39.5% for 25, 50, and 100 mg/L dye concentration, respectively (Figure 4). An interesting result was observed that at least 60% of dyes uptake was achieved in a very short contact time of 1 min for 25 mg/L dye concentration. The adsorption capacity of RB19 dye increased over time and reached a maximum value at 60 min. After this time, the adsorption capacity reached a constant value indicating that no more dye molecules were further removed from the solution (Figure 4). The result implied there was a high affinity between dye molecules and Terra Rosa soil at low dye concentration.

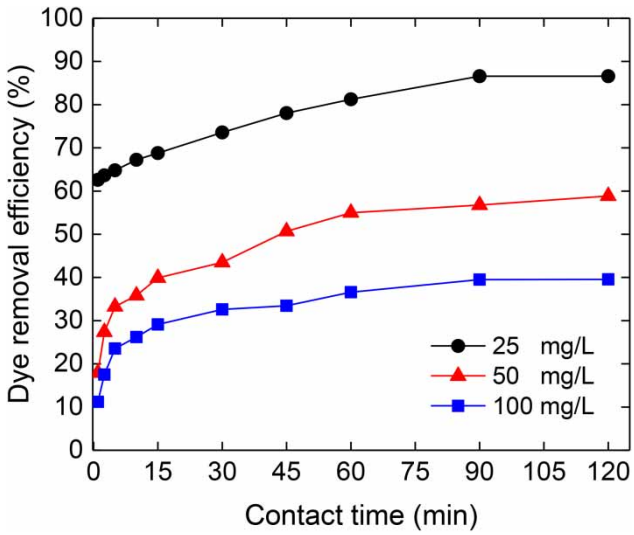

Figure 4 | Effect of initial dye concentration (25–100 mg/L) and contact time (5–120 min) on the RB19 dye removal by Terra Rosa soil (pH, 2; soil loading, 10 g/L; contact time, 120 min).

The calculated kinetic parameters and constants are listed in Table 3. The experimental data showed good compliance with the pseudo second-order kinetic model in terms of higher correlation coefficients ($R^2 > 0.99$). Increasing of the initial dye concentration from 25 to 100 mg/L, the adsorbed amount of dye increased from 2.38 to 3.81 mg/g. This can be explained as increasing in the driving force of the concentration can overcome mass transfer resistance of dye molecules between the aqueous and solid phases. Therefore, a higher initial dye concentration may increase the adsorption capacity (Demirbas *et al.* 2009).

The values of the second order rate constants (k_2) decreased from 0.143 to 0.049 g/mg·min when initial dye concentration increased from 25 to 100 mg/L, which indicated the adsorption process was highly concentration dependent (Table 3). Lower concentration of dye molecules in the aqueous solution might cause lower collisions among dye molecules, therefore dye molecules could be bonded faster to the soil's active sites.

The values of the rate constant (k_{id}) from Weber–Morris kinetic model was increased from 0.074 to 0.150 mg/g·min$^{1/2}$ when initial dye concentration was increased from 25 to 100 mg/L. Hence, dye concentration in the aqueous solution had a mild influence on both the adsorption diffusion kinetics and the mechanism controlling the kinetic coefficient. At high initial concentrations, the concentration gradient generated between the solution and the surface of the soil particle leads to enhanced dye molecules' diffusion through the film surrounding the particle and into the micro-porous structure of the soil (Dizge *et al.* 2009).

Table 3 | The adsorption kinetic parameters of RB19 dye at different initial dye concentrations

Parameters	Pseudo-first-order				Pseudo-second-order				Elovich			Weber–Morris		
Initial dye concentration (mg/L)	$q_{e,exp.}$ (mg/g)	$q_{e,cal.}$ (mg/g)	k_1 (1/min)	r^2	$q_{e,exp.}$ (mg/g)	$q_{e,cal..}$ (mg/g)	k_2 (g/mg·min)	r^2	α (mg/g·min)	β (g/mg)	r^2	k_{id} (mg/g min$^{1/2}$)	I (mg/g)	r^2
25	2.38	1.44	0.025	0.993	2.38	2.41	0.143	0.998	26.79	6.63	0.891	0.074	1.63	0.958
50	2.68	1.55	0.032	0.978	2.68	2.75	0.060	0.995	4.89	2.60	0.984	0.128	1.36	0.925
100	3.81	2.95	0.057	0.863	3.81	3.93	0.049	0.997	5.19	1.77	0.989	0.150	2.27	0.951

Adsorption isotherm and thermodynamic analysis

The adsorption isotherm was studied to determine the relationship between capacity of soil and the equilibrium concentration of dye in the aqueous phase. Three isotherm models (Langmuir, Freundlich, Temkin) were tested. Figure 5 represents the plotted models and the isotherm constant is shown in Table 4. The results indicated that the r^2 value of the Langmuir plot is higher than the other models (Figure 5(a)). Therefore, dye molecules are accepted to be adsorbed as a monolayer on adsorption sites of soil. The maximum capacity of soil was found to be 4.11 mg/g. Additionally, the Freundlich constant (n) is between 1 and 10, which proves that Terra Rosa soil is a favorable adsorbent for RB19 dye (Figure 5(b)). Table 4 also shows that low correlation was obtained with the Temkin isotherm ($r^2 = 0.655$). According to Figure 5(c), the Temkin adsorption potential ($A = 24.91$ L/g, $B = 0.494$ J/mol) is an indication of the heat of sorption between dye molecules and soil surface. This indicated that the heat of adsorption

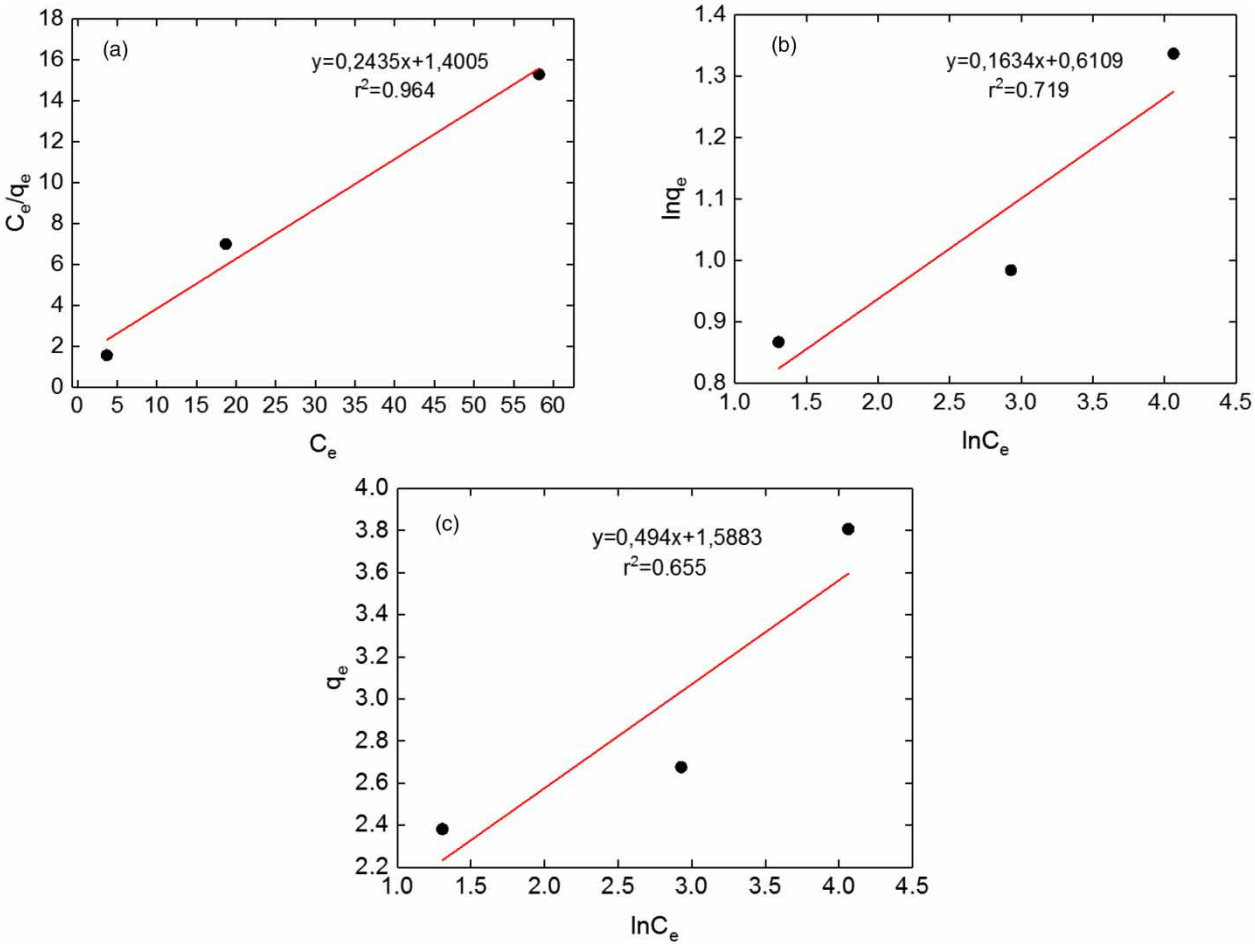

Figure 5 | The linear plot of Langmuir (a), Freundlich (b), Temkin (c) equilibrium model.

Table 4 | The isotherm parameters of RB19 dye adsorption by Terra Rosa soil

Langmuir constant			Freundlich constant			Temkin constant		
Q_o (mg/g)	b (L/mg)	r^2	n	k_f (mg/g)	r^2	B (J/mol)	A (L/g)	r^2
4.11	0.17	0.964	6.12	4.07	0.719	0.49	24.91	0.655

of RB19 dye molecules onto the surface of soil particles decreased with increasing temperature from 293 to 313 K and the sorption is exothermic. Also, the b value (5.01 kJ/mol) indicated a weak interaction between dye molecules and soil particles, supporting an ion-exchange mechanism for the present study (Shahmohammadi-Kalalagh *et al.* 2011).

The thermodynamic model enhances the calculation of enthalpy, entropy, and Gibbs free energy change. Thermodynamic parameters were calculated using the following equations.

Enthalpy (ΔH^o) and entropy (ΔS^o) change:

$$\log K = \frac{\Delta S^o}{2.303\,R} - \frac{\Delta H^o}{2.303\,R}\left(\frac{1}{T}\right) \quad (10)$$

ΔH^o and ΔS^o changes were found from the slope and intercept of the plot of logK as a function of 1/T, respectively.

Gibbs free energy (ΔG^o) change:

$$\Delta G = -2.303 \times R \times T \times \log K \quad (11)$$

where K (=b) is the adsorption isotherm constant, R is the gas constant (8.314 J/K·mol), T is the absolute temperature (K).

The thermodynamic studies were carried out at 293, 303, and 313 K with initial dye concentration of 25 mg/L, adsorbent dosage of 10 g/L, and pH 2. The thermodynamic results are shown in Table 5. The negative value of the change in enthalpy (−50.81 kJ/mol) indicated that the adsorption was physico-chemical in nature and also exothermic, thereby demonstrating that the process was stable energetically. The negative entropy change (ΔS^o) value (−0.18 kJ/mol·K) corresponds to a decrease in randomness at the solid–liquid interface. The positive Gibbs free energy (ΔG^o) indicated the reaction was not feasible at this temperature and the reaction was reversible.

Table 5 | Values of thermodynamic parameters for adsorption of RB19 dye on Terra Rosa soil

	T (K)		
	293	303	313
K_c	0.47	0.27	0.13
ΔG^o (kJ/mol)	1.84	3.18	5.39
ΔH^o (kJ/mol)	− 50.81		
ΔS^o (kJ/mol·K)	− 0.18		

Heterogeneous Fenton studies

In this study, the heterogeneous Fenton reaction was tested because the iron content of the Terra Rosa was high and the highest adsorption efficiency (86.6%) was obtained at pH 2. Therefore, pH (2) and temperature (25 ± 1 °C) were kept constant and the effect of soil loading (1, 5, 10, 20 g/L) and H_2O_2 dosage (10, 20, 50 mM) was solely tested on the decolorization of RB19 at 50 mg/L dye concentration (Figure 6).

Results in Figure 6(a) indicate that increasing soil loading from 1 to 10 g/L increased the dye removal (from 68.1 to 90.0%) but further rise to 20 g/L had significant drop on dye removal (71.9%). Because increasing soil loading provided additional surface area for adsorption and an additional amount of Fe ions for the formation of OH• radicals, however, further increase in the iron rich soil amount significantly decreased the color removal efficiency, which could be attributed to the inhibition effect caused by excess iron ions in the heterogeneous Fenton reaction that acted as scavengers as shown by Equation (12) (Merlain *et al.* 2016).

$$Fe^{2+} + OH\bullet \rightarrow Fe^{3+} + OH^- \quad (12)$$

On the contrary, increasing H_2O_2 dosage from 0 to 50 mM had adverse effect on dye removal (from 27.5 to 62.6%) and significant drop occurred when 50 mM dosage was used (Figure 6(b)). Since 10 mM H_2O_2 dosage was sufficient for stoichiometric reaction and excess H_2O_2 dosage caused OH• radical quencher, consequently lowering the OH• radical concentration (Equations (13) and (14)). Muruganandham *et al*. also confirmed that excess H_2O_2 acted as OH• radical quencher when photochemical oxidation of reactive azo dye with UV–H_2O_2 process was performed (Muruganandham & Swaminathan 2004). The same effect was also observed when heterogeneous photo-Fenton oxidation of reactive azo dye solutions using iron exchanged zeolite catalyst was used (Tekbas *et al.* 2008).

$$H_2O_2 + OH\bullet \rightarrow HO_2^\bullet + H_2O \quad (13)$$

$$H_2O_2^\bullet + OH\bullet \rightarrow H_2O + O_2 \quad (14)$$

To demonstrate that the process is considered as essentially heterogeneous, leached iron concentrations into the solution were measured in 60 min final time and found less than 0.2 mg/L. Hence, this amount was very small considering the iron content of the soil loading.

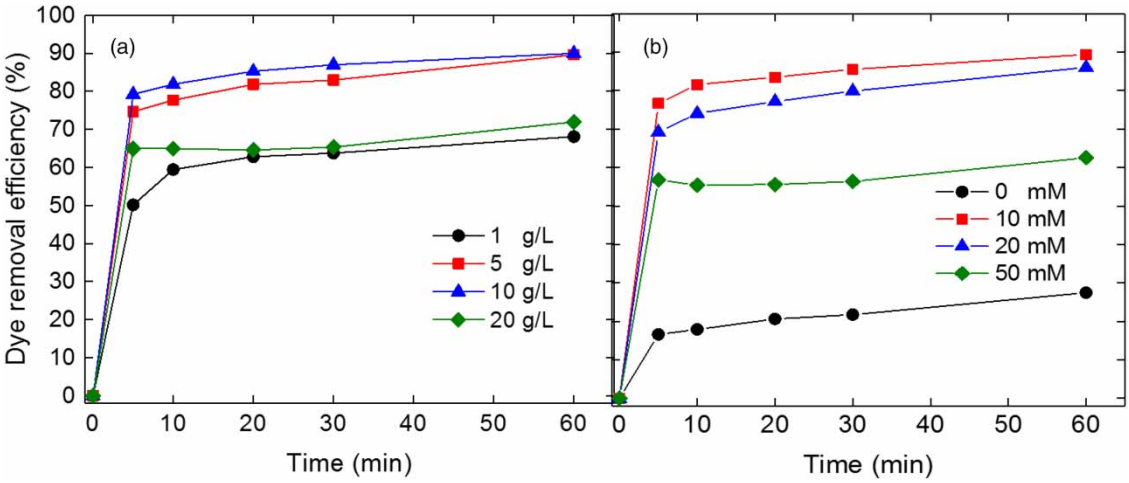

Figure 6 | (a) Effect of soil loading (pH, 2; H_2O_2 dosage, 20 mM; initial dye volume and concentration, 250 mL and 50 mg/L; temperature, 25 ± 1 °C) and (b) H_2O_2 dosage (pH, 2; soil loading, 5 g/L; initial dye volume and concentration, 250 mL and 50 mg/L; temperature, 25 ± 1 °C) on the removal of RB 19 dye by Fenton reaction.

Adsorbent characterization before and after the adsorption and Fenton process

XRF analysis was performed to know chemical composition of the minerals in raw soil, after adsorption and Fenton oxidation (Table 6). Alumina, silica, and iron oxides were the major component and the others were trace quantities. Some components' values, such as NiO, ZnO, Rb_2O, SrO and ZrO_2, were below detection limits after adsorption process. According to the table, clay and hematite minerals were the major component of samples mineralogically.

The FTIR spectra analysis of raw soil, after adsorption and Fenton oxidation are shown in Table 7. The FTIR spectra revealed that various functional groups were detected on the surface of soil. There were some peaks that had shifted

Table 6 | XRF analyses of raw soil, after adsorption and Fenton oxidation

Chemical composition	Raw soil (weight %)	After adsorption (weight %)	After Fenton (weight %)
Na_2O	0.266	0.670	0.370
MgO	3.005	2.320	2.827
Al_2O_3	21.777	22.020	21.995
SiO_2	54.305	54.640	54.304
P_2O_5	0.238	0.230	0.235
SO_3	0.235	0.431	0.254
Cl	0.104	0.140	0.124
K_2O	3.223	3.050	3.115
CaO	2.643	2.480	2.580
TiO_2	1.530	1.450	1.525
Cr_2O_3	0.041	0.280	0.045
MnO	0.230	0.029	0.222
Fe_2O_3	12.254	12.260	12.260
NiO	0.034	–	0.032
ZnO	0.032	–	0.030
Rb_2O	0.019	–	0.017
SrO	0.021	–	0.020
ZrO_2	0.045	–	0.045

Table 7 | FTIR analyses of raw soil after adsorption and Fenton oxidation

Raw soil (cm^{-1})	After adsorption (cm^{-1})	After Fenton (cm^{-1})	Description
3,697	3,697	3,697	Al–O–H stretching
3,620	3,622	3,621	Al–O–H (inter-octahedral)
–	2,972	2,981	Symmetric C-H stretching
1,635	1,637	1,636	H–O–H stretching
912	912	912	Al–O–H stretching
797	797	797	Si–O stretching. Si–O–Al stretching. (Al. Mg)–O–H
778	779	779	Si-O stretching
693	693	693	Si–O stretching. Si–O–Al stretching
527	531	531	C–O. C–C out of plane bending
467	467	469	Si–O stretching. Si–O–Fe stretching

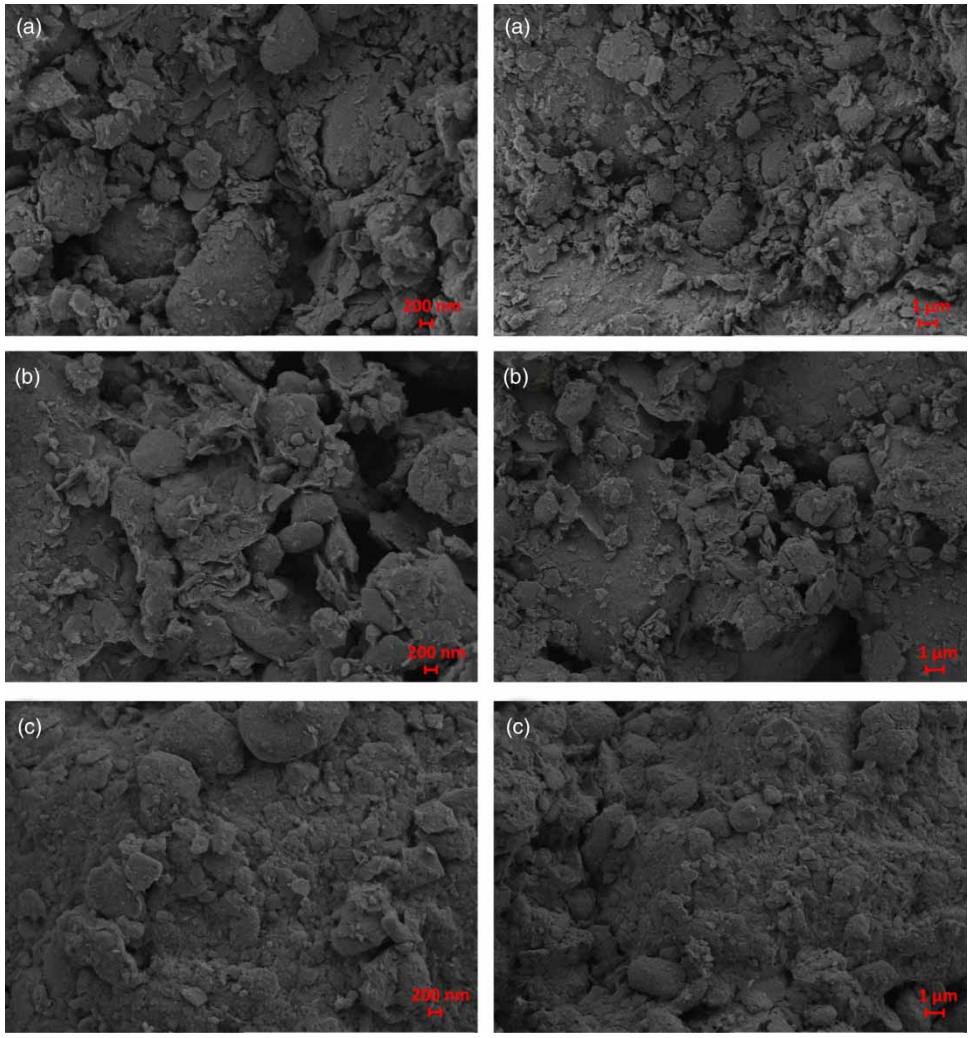

Figure 7 | SEM analyses of Terra Rosa soil before adsorption (a), after adsorption (b), and after Fenton reaction (c) (200 nm and 1 μm magnification).

or disappeared and new peaks were also detected in the RB19 adsorbed dye by Terra Rosa. According to FTIR analyses, OH-stretching fundamental spectrums were 3,694 cm^{-1} and 3,620 cm^{-1} at hydroxyl groups with alumina. After adsorption and Fenton reactions, a new spectrum was observed about 2,970 cm^{-1}. Si-O stretching can be observed at about 1,000 cm^{-1}. Major spectrums and the fingerprints showed that Terra Rosa soil mineralogically contained Mont-morillonit, hematite and quartz minerals.

The SEM of the raw soil was compared after adsorption and Fenton oxidation process (Figure 7). The aggregations were seen when raw and after adsorption while it decreased after Fenton oxidation.

RB19 dye decolorization using Terra Rosa soil is shown in Figure 8. It was clearly seen from the figure that pH of aqueous solution was important to decolorize RB19 dye

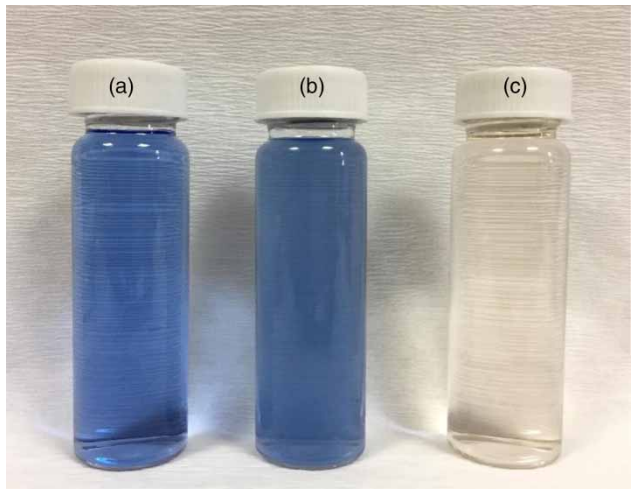

Figure 8 | RB19 dye decolorization by Terra Rosa adsorbent (a) pH 2 dye solution before adsorption, (b) pH 5.3 dye solution after adsorption, (c) pH 2 dye solution after adsorption.

Table 8 | Comparison of recently published literature on RB19 dye removal by different adsorbents

Adsorbent	pH	Kinetic model	Isotherm model	Adsorption capacity (mg/g)	Reference
Terra Rosa soil	2	Pseudo-second order	Langmuir isotherm	4.11	This study
Macrophyte *Salvinia natans*	1	Pseudo-second order	Langmuir isotherm	61.90	Pelosi *et al.* (2014)
Pineapple leaf powder and lime peel powder	–	Pseudo-second order	Langmuir isotherm	9.58	Rahmat *et al.* (2016)
Orange peel	–	–	Langmuir and Freundlich isotherm	11.62	Mafra *et al.* (2013)

using Terra Rosa soil. The photo on the left belongs to pH 2 dye solution before adsorption process. The photo on the right belongs to pH 2 dye solution after adsorption process whereas no effect was observed at pH 5.3 (original pH) (middle photo).

Several studies have been performed using various types of adsorbents for RB19 dye adsorption. Table 8 summarizes a comparison of some recent publication for optimum adsorption conditions and maximum capacity. Terra Rosa soil showed comparable adsorption capacity with respect to other adsorbents, revealing that soil is an attractive, feasible, and novel low-cost adsorbent.

CONCLUSIONS

In the present work, Terra Rosa soil was investigated for the removal of RB19 dye from aqueous solution. Adsorption experiments showed that the adsorption of RB 19 dye by soil was favorable under highly acidic conditions. Pseudo-second-order and Langmuir models fit the kinetic and equilibrium experimental data, respectively. The maximum adsorption capacity was found to be 3.81 mg/g. Moreover, the heterogeneous Fenton reaction was tested because the iron content of the Terra Rosa was high and the highest dye removal efficiency (89.4%) was obtained at pH 2. The Fenton studies indicated that increasing soil loading caused increase of dye removal up to 10 g/L but further rise to 20 g/L had significant drop on dye removal. However, increasing H_2O_2 dosage had an adverse effect on dye removal and significant drop was detected. As a result, Terra Rosa soil can be considered as an efficient, inert, nontoxic, environmentally friendly, easily available, and economical adsorbent for industrial applications.

ACKNOWLEDGEMENTS

This study was supported by the Research Fund of Mersin University in Turkey with Project Number: 2017-1-AP4-2212.

REFERENCES

Al-Ghouti, M. A., Khraisheh, M. A. M., Allen, S. J. & Ahmad, M. N. 2003 The removal of dyes from textile wastewater: a study of the physical characteristics and adsorption mechanisms of diatomaceous earth. *J. Environ. Manage.* **69**, 229–238.

Allen, S. J., Mckay, G. & Porter, J. F. 2004 Adsorption isotherm models for basic dye adsorption by peat in single and binary component systems. *J. Colloid Interface Sci.* **280** (2), 322–333.

Bangash, F. K. & Alam, S. 2009 Adsorption of acid blue 1 on activated carbon produced from the wood of Ailanthus altissima. *Brazilian J. Chem. Eng.* **26**, 275–285.

Boero, V. & Schwertmann, U. 1989 Iron oxide mineralogy of terra rossa and its genetic implications. *Geoderma* **44**, 319–327.

Boero, V., Premoli, A., Melis, P., Barberis, E. & Arduino, E. 1992 Influence of climate on the iron oxide mineralogy of terra rossa. *Clays & Clay Minerals* **40** (1), 8–13.

Bronger, A., Ensling, J., GiJtlich, P. & Spiering, H. 1983 Rubification of terrae rossae in Slovakia: a m6ssbauer effect study. *Clays & Clay Minerals* **31**, 269–276.

Demirbas, E., Dizge, N., Sulak, M. T. & Kobya, M. 2009 Adsorption kinetics and equilibrium of copper from aqueous solutions using hazelnut shell activated carbon. *Chem. Eng. J.* **148**, 480–487.

Dizge, N., Keskinler, B. & Barlas, H. 2009 Sorption of Ni(II) ions from aqueous solution by Lewatit cation-exchange resin. *J. Hazard. Mater.* **167**, 915–926.

Durn, G., Miko, S., Čović, M., Barudžija, U., Tadej, N., Namjesnik-Dejanović, K. & Palinkaš, L. 1999 Distribution and behaviour of selected elements in soil developed over a historical Pb-Ag mining site at Sv. Jakob, Croatia. *J. Geochem. Exploration* **67**, 361–376.

Fil, B. A., Yilmaz, M. T., Bayar, S. & Elkoca, M. T. 2014 Investigation of adsorption of the dyestuff astrazon red violet 3rn (basic violet 16) on montmorillonite clay. *Brazilian J. Chem. Eng.* **31** (01), 171–182.

Gordon, P. F. & Gregory, P. 1987 *Anthraquinone Dyes*. Chapter 4. Organic Chemistry in Colour, Part of the series Springer Study Edition. Berlin, Germany, pp. 163–199.

Guaratini, C. C. & Zanoni, M. V. B. 2000 Textile dyes. *Quim. Nova* **23**, 71–78.

Günal, H. 2006 Pedogenesis and classification of soils located on two consecutive topographies. *Gaziosmanpaşa Üniversitesi Ziraat Fakültesi Dergisi* **23** (2), 59–68.

Ho, Y. S., Porter, J. F. & McKay, G. 2002 Equilibrium isotherm studies for the sorption of divalent metal ions onto peat: copper, nickel and lead single component systems. *Water Air Soil Pollut.* **141**, 1–33.

Kubiena, W. L. 1953 *The Soils of Europe*. Thomas Murby, London.

Li, Y., Zhang, X., Yang, R., Li, G. & Hu, C. 2016 Removal of dyes from aqueous solutions using activated carbon prepared from rice husk residue. *Water Sci. Tech.* **73** (5), 1122–1128.

Low, K. S., Lee, C. K. & Tan, B. F. 2000 Quaternised wood as sorbent for reactive dyes. *Appl. Biochem. Biotechnol.* **87**, 233–245.

Mafra, M. R., Igarashi-Mafra, L., Zuim, D. R., Vasques, É. C. & Ferreira, M. A. 2013 Adsorption of Remazol Brilliant Blue on an orange peel adsorbent. *Brazilian J. Chem. Eng.* **30** (03), 657–665.

Merlain, T. G., Nanganoa, L. T., Desire, B. B. P., Nsami, N. J. & Mbadcam, K. J. 2016 Fenton-like oxidation of Acid Yellow 23 in the presence of iron rich soil. *Adv. Chem. Eng. Sci.* **6**, 553–569.

Moreira, R. F. P. M., Soares, J. L., José, H. J. & Rodrigues, A. E. 2001 The removal of reactive dyes using high-ash char. *Brazilian J. Chem. Eng.* **18**, 327–336.

Murali, R., Murthy, C. N. & Sengupta, R. A. 2015 Adsorption studies of toxic metals and dyes on soil colloids and their transport in natural porous media. *Int. J. Environ. Sci. Technol.* **12**, 3563–3574.

Muruganandham, M. & Swaminathan, M. 2004 Photochemical oxidation of reactive azo dye with UV–H_2O_2 process. *Dyes and Pigments* **62**, 269–275.

Ncibi, M. C., Hamissa, B. A. M., Fathallah, A., Kortas, M. H., Baklouti, T., Mahjoub, B. & Seffen, M. 2009 Biosorptive uptake of methylene blue using Mediterranean green alga *Enteromorpha* spp. *J. Hazard. Mater.* **170**, 1050–1055.

Pelosi, B. T., Lima, L. K. S. & Vieira, M. G. A. 2014 Removal of the synthetic dye Remazol Brilliant Blue R from textile industry wastewaters by biosorption on the macrophyte *Salvinia natans*. *Brazilian J. Chem. Eng.* **31**, 1035–1045.

Rahmat, N. A., Ali, A. A., Salmiati, N., Hussain, M. S., Muhamad, R. A. & Hadibarata, K. T. 2016 Removal of Remazol Brilliant Blue R from aqueous solution by adsorption using pineapple leaf powder and lime peel powder. *Water Air Soil Pollut.* **227**, 105–115.

Rani, K. C., Naik, A., Chaurasiya, R. S. & Raghavarao, K. S. M. S. 2017 Removal of toxic Congo red dye from water employing low-cost coconut residual fiber. *Water Sci. Tech.* **75** (9), 2225–2236.

Rattan, V. K., Purai, A., Singh, Ha. & Manoochehri, M. 2008 Adsorption of dyes from aqueous solution by cow dung ash. *Carbon Letters* **9** (1), 1–7.

Russiarani, S. & Balakrishanan, K. 2015 Adsorptıon of methylene blue dye on termite soil. *Int. J. Biosci. Nanosci.* **2** (8), 175–184.

Shahmohammadi-Kalalagh, S., Babazadeh, H., Nazemi, A. & Manshouri, M. 2011 Isotherm and kinetic studies on adsorption of Pb, Zn and Cu by kaolinite. *Caspian Journal of Environmental Sciences* **9**, 243–255.

Silva, L. G., Ruggiero, R., Gontijo, P. M., Pinto, R. B., Royer, B., Lima, E. C., Fernandes, T. H. M. & Calvete, T. 2011 Adsorption of Brilliant Red 2BE dye from water solutions by a chemically modified sugarcane bagasse lignin. *Chem. Eng. J.* **168**, 620–628.

Sivaraj, R., Namasivayam, C. & Kadirvelu, K. 2001 Orange peel as an adsorbent in the removal of acid violet 17 (acid dye) from aqueous solutions. *Waste Manag.* **21**, 105–110.

Tekbas, M., Yatmaz, H. C. & Bektas, N. 2008 Heterogeneous photo-Fenton oxidation of reactive azo dye solutions using iron exchanged zeolite as a catalyst. *Microporous and Mesoporous Materials* **115**, 594–602.

Torrent, J. & Cabedo, A. 1986 Sources of iron oxides in reddish brown soil profiles from calcarenites in southern Spain. *Geoderma* **37**, 57–66.

Yaalon, D. H. 1997 Soils in the Mediterranean region: what makes them different? *Catena* **28**, 157–169.

First received 28 February 2017; accepted in revised form 4 August 2017. Available online 4 September 2017